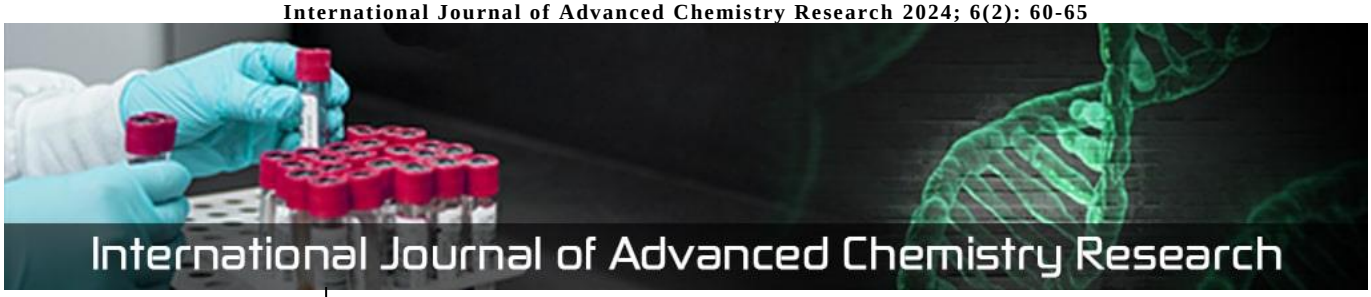

ISSN Print: 2664-6781
ISSN Online: 2664-679X
IJACR 2024; 6(2): 60-65
www.chemistryjournals.net
Received: 02-07-2024
Accepted: 05-08-2024

Rajesh Kumar
Research Scholar, PG department of Chemistry Ranchi University Ranchi Jharkhand, India

Rudhima Raj
Research Scholar, PG department of Chemistry Ranchi University Ranchi Jharkhand, India

Smriti Singh
Smriti Singh, Assistant Professor PG Department of Chemistry Ranchi University Ranchi Jharkhand, India

Corresponding Author:
Smriti Singh
Assistant Professor PG Department of Chemistry Ranchi University Ranchi Jharkhand, India

Enhanced photo catalytic properties for environmental applications of non-metal doped nickel oxide

Rajesh Kumar, Rudhima Raj and Smriti Singh

DOI: https://doi.org/10.33545/26646781.2024.v6.i2a.229

Abstract
This study investigates the process of hydrothermal synthesis to create a nano-composite (NiO-BS-GO) by incorporating boron (B) and Sulfur (S) into nickel oxide (NiO) together with Graphene oxide (GO). The resulting nanocomposite exhibits improved photocatalytic characteristics. The combination demonstrated a substantial enhancement in both optical and photocatalytic degradation of methylene blue (MB) and rhodamine B (RhB) when exposed to visible light. This improvement is credited to the greater surface area, enhanced charge separation, and increased absorption of visible light. The nanocomposite composed of NiO-BS-GO exhibited remarkable stability and reusability, indicating its promising suitability for environmental remediation purposes.

Keywords: Photocatalytic activity, nanocomposites, nickel oxide (NiO), doping, boron sulfur, graphene oxide

Introduction

Water pollution is a pressing environmental problem that requires effective photocatalysts for treating wastewater [1-4]. Nickel oxide (NiO) exhibits potential, but its photocatalytic activity needs enhancement. The characteristics can be enhanced by doping NiO with boron (B) and sulfur (S) and adding graphene oxide (GO) [5-6]. Water is an essential and diverse feature for all living organisms, and contamination of water resources demands careful consideration [7-8]. Industrial effluent, including pesticides, herbicides, dyes, and organic pollutants, is a significant source of water pollution [9-11]. Even trivial amounts of these pollutants can significantly impact ecosystems and contribute to climate change [12]. The dyeing processes and various industrial activities release effluents containing colorful, non-biodegradable, and hazardous chemicals. Such wastewater is a major contributor to methane emissions (about 10%), leading to global warming. Thus, treating wastewater before its release into rivers is imperative to minimize environmental damage. Non-biodegradable chemicals and soluble dyes are among the primary causes of water pollution [13, 14].

Due to overcrowding, food consumption, and industrialization, water pollution is rising [15, 16]. In developing countries, lakes and rivers are heavily contaminated, making this problem worse. Water shortages and microbiological and chemical pollution plague many rural communities. The UNO estimates that 50% of impoverished nations' populations suffer from health issues from dirty drinking water. Even though the world possesses 3% freshwater reserves, only 0.01% is appropriate for human use, and waterborne illnesses kill 5 million people annually [17-19]. As population grows, freshwater scarcity for sustainable living becomes a serious challenge [20].

Graphene oxide (GO) is ideal for visible-light-responsive nanocomposites. Because GO speeds up light-induced charge carrier recombination [21-26]. Graphene oxide (GO) accepts electrons from copper sulfide's conduction band [27-29]. This mechanism slows recombination by lengthening electron paths [30]. When boron (B) is doped into the π-framework of GO, flaws increase its surface area, generating more adsorptive sites for pollutant molecules [31-33]. Doped graphene oxide contains nitrogen, phosphorus, iodine, and boron [34-35].

Boron doping is notable because its size matches graphene oxide, allowing it to fit into the lattice structure and increase charge resistance [36-38].

BGO has been intensively explored for its potential in environmental and energy applications because boron adds active sites around graphene oxide's edges [39, 40]. Photo catalytic pollutant breakdown using B-doped graphene oxide and semiconductor materials has received little attention [41-44]. Because graphene oxide is selectively doped with non-metal atoms. BGO-based nanocomposites' ability to degrade pollutants needs further study [45-48].

This study shows a very efficient two-step technique for creating BGO-CuS by doping carbon-based graphene oxide (GO) with non-metal (B) and linking it with CuS via hydrothermal synthesis [49-53]. The novel nanocatalyst was tested for its photocatalytic breakdown of methylene blue (MB) in sunshine [54-56]. Boron as a dopant in graphene oxide reduced the bandgap and increased electrical conductivity. The initiative seeks to build a photocatalyst that increases photocatalytic activity under sunlight [57-58].

Materials and Methods

Synthesis of NiO/GO composite with B and S doping

The composite was fabricated by a hydrothermal technique: Combine 1.5 grams of nickel nitrate hexahydrate ($Ni(NO_3)_2 \cdot 6H_2O$), 0.2 grams of boric acid (H_3BO_3), and 0.3 grams of thiourea (CH_4N_2S) in 40 milliliters of deionized water. Introduce 0.5 grams of graphene oxide (GO) and subject it to ultra-sonication for a duration of 30 minutes. Place the mixture into a Teflon-lined autoclave with a capacity of 100 mL and heat it at a temperature of 180 °C for a duration of 12 hours. Rinse the product using deionized water and ethanol, followed by drying at a temperature of 60 °C for duration of 24 hours [59-62].

Characterization Techniques

Technique	Main Information Derived	Remark
XRD	Crystal structure, composition, grain size	Limited for amorphous materials
XAS	Chemical state, interatomic distances	Requires synchrotron sources
SAXS	Particle size, distribution, growth kinetics	Lower resolution, good for in-situ analysis
TEM	Size, morphology, crystal structure	High-resolution, extensive sample preparation
SEM	Surface morphology, elemental composition	Quick imaging, less effective for bulk analysis
XPS	Surface chemical states, elemental composition	Ultra-high vacuum required, surface-focused
FTIR	Surface composition, ligand binding	Limited structural information
SQUID	Magnetization, blocking temperature	Complex equipment, high sensitivity
VSM	Magnetization through M–H plots, ZFC-FC curves	Similar to SQUID, less accessible

Parameter	Techniques Suitable
Size	TEM, XRD, DLS, SAXS, SEM, AFM
Shape	TEM, HRTEM, AFM, FMR
Elemental Composition	XRD, XPS, ICP-MS, SEM-EDX
Crystal Structure	XRD, EXAFS, HRTEM, electron diffraction
Size Distribution	DCS, DLS, SAXS, NTA, ICP-MS
Chemical State	XAS, EELS, XPS, Mössbauer
Growth Kinetics	SAXS, NMR, TEM
Surface Composition	XPS, FTIR, NMR, SIMS
Surface Area	BET, liquid NMR
Surface Charge	Zeta potential, EPM
Concentration	ICP-MS, UV-Vis
Agglomeration State	Zeta potential, DLS, SEM
Density	DCS, RMM-MEMS
Single Particle Properties	Sp-ICP-MS, HRTEM, liquid TEM
3D Visualization	3D-tomography, AFM, SEM
Dispersion in Matrices	SEM, AFM, TEM
Structural Defects	HRTEM, EBSD
Detection of NPs	TEM, SEM, STEM
Optical Properties	UV-Vis-NIR, PL, EELS-STEM
Magnetic Properties	SQUID, VSM, Mössbauer, FMR

The XRD patterns verified the presence of a face-centered cubic structure in NiO, along with extra peaks suggesting the successful doping of B and S, as well as the presence of GO. The scanning electron microscope (SEM) images revealed that the NiO-BS-GO composite possesses a sheet-like structure, which is distinct from the spherical shape of pure NiO.

The presence of Ni, B, S, O, and carbon (from GO) was confirmed using EDX analysis. The UV-vis spectroscopy analysis showed that the composite material had a reduced band gap energy, which suggests that it has an improved ability to absorb visible light.

BET Analysis and Optical Analysis of Nanocomposites

The specific surface area of nanocomposites such as NiO-BS-GO can be determined using nitrogen gas adsorption data and the Brunauer–Emmett–Teller (BET) method. In a study, the BET surface areas of these nanocomposites were found to be 25.24 m^2/g. This high surface area indicates that doping results in a significant increase in surface area.

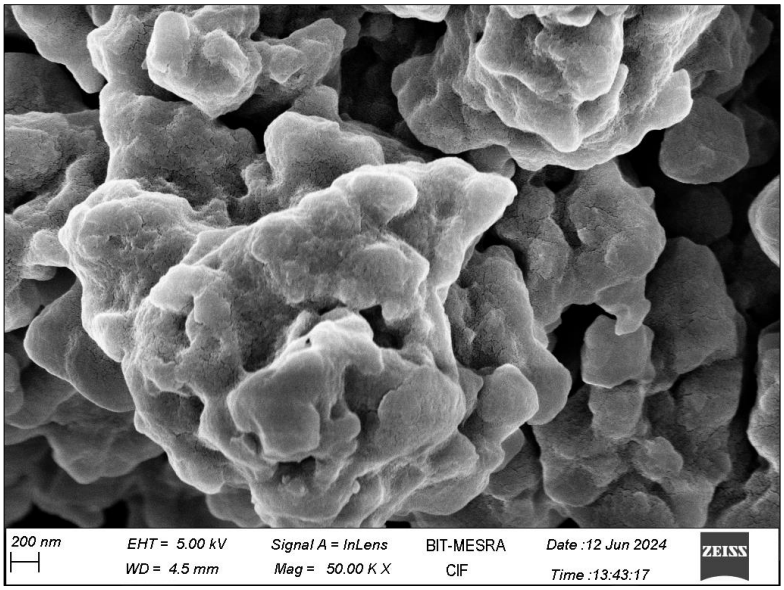

Fig 1: FESEM image of Nickel oxide doped with Boron and Sulphur and GO

Result

Photo catalytic activity: The assessment of photo catalytic activity involved the degradation of methylene blue (MB) using visible light irradiation. Distribute 50 milligrams of the photo catalyst evenly in 100 mL of MB solution with a concentration of 10 mg/L. Agitate in darkness for a duration of 30 minutes to achieve a state of adsorption-desorption equilibrium. Expose to radiation using a 300 W Xenon lamp equipped with a visible light filter. Extract 5 mL samples at consistent time intervals, subject them to centrifugation, then evaluate them using a UV-vis spectrophotometer.

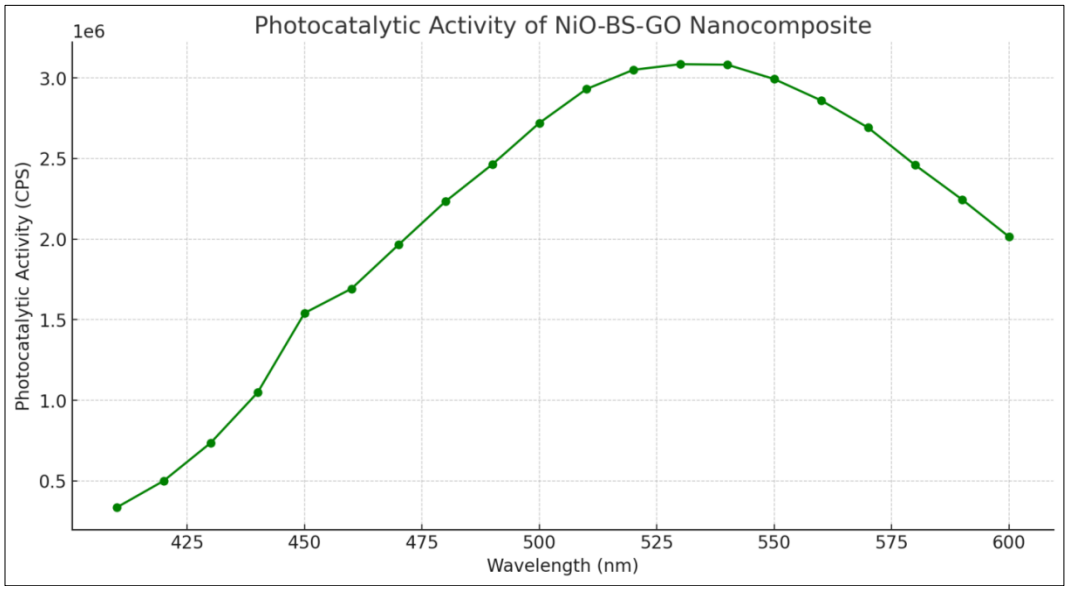

Fig 2: Photocatalytic activity of NiO-BS-GO nanocomposite

The relationship between doping and structural integrit

The structural stability of NiO can be enhanced by doping it with Boron (B) and Sulfur (S). The substitution of nickel and oxygen atoms in the NiO lattice with boron and sulfur atoms results in the formation of a stronger structure that exhibits enhanced resistance to deterioration over time. The use of Graphene Oxide (GO) creates a robust and pliable framework that sustains the NiO particles. Graphene oxide (GO) sheets function as a framework, preventing the clustering of NiO particles and preserving a large surface area, which is essential for efficient photocatalytic performance.

Enhanced Electrical Charge Division and Decreased Combination of Charges

The process of charge separation is enhanced by the combination of B and S doping and the integration of GO, resulting in improved charge separation. The recombination of electrons and holes in photo catalysis is mitigated due to the presence of dopants, which induce localized states that effectively capture and immobilize the charge carriers. Enhanced Electron Transfer: The inclusion of GO improves the channel for electron transfer, hence diminishing the likelihood of electron-hole recombination. As a result, this enhances the efficiency of photo catalytic activities and extends the effective lifespan of the material.

Increased Surface Area and Catalytic Sites

The Nano composite structure, consisting of graphene oxide (GO) sheets dispersed with nickel oxide (NiO) particles, offers an expanded surface area. This guarantees the presence of a greater number of active sites for photo catalytic processes, hence improving both the overall activity and stability. Catalytic sites are formed by the introduction of dopants and graphene oxide (GO). These sites exhibit enhanced reactivity and stability by effectively inhibiting the sintering or agglomeration of NiO particles, hence preserving the active surface area.

Photocorrosion resistance

Photocorrosion Resistance: The addition of boron (B) and sulfur (S) to NiO improves its ability to resist photocorrosion. Photocorrosion is a prevalent problem in photo catalysts, characterized by the deterioration of the material due to extended exposure to light. Dopants serve to enhance the stability of the NiO lattice, hence reducing its vulnerability to photo corrosion.

GO Protection: Graphene oxide (GO) functions as a protective barrier that absorbs a portion of the photogenerated holes, thereby diminishing the oxidative stress on nickel oxide (NiO) particles. This defensive mechanism additionally improves the resilience of the composite.

Discussion

Due to its photocatalytic and stability, the NiO-BS-GO nanocomposite is a diverse and powerful environmental solution. Multiple applications of this sophisticated material have shown remarkable efficiency, contributing to environmental sustainability.

It can be used in following applications

1. **Aquatic Filtration and Effluent Processing:** The nanocomposite effectively remediates industrial and municipal wastewater by degrading organic pollutants including colors and medications. Its visible light photocatalytic activity breaks down persistent organic pollutants (POPs), minimizing their environmental impact.
2. **Air Purification:** NiO-BS-GO decomposes VOCs from industrial operations, cars, and domestic objects, reducing indoor and outdoor air pollution. It improves air quality by degrading NOx and SOx emissions in ventilation systems.
3. **Solar-Powered Disinfection:** The nanocomposite's photocatalytic capabilities enable pathogen inactivation in fluids and surfaces. It is essential for purifying water and maintaining cleanliness in remote and disaster-stricken places.
4. **Soil Remediation:** NiO-BS-GO effectively treats organic and heavy metal-contaminated soils. It breaks down complex organic pollutants to bioremediate damaged places and restore soil.
5. **Environmental Sensing and Monitoring:** The material's sensitivity to environmental changes enables detection and monitoring, enhancing environmental management and protection.
6. **Power Generation:** NiO-BS-GO's effective conversion of visible light into chemical energy enables hydrogen synthesis via water splitting. This approach promotes sustainable energy and reduces pollution and energy shortages.
7. **Sustainable Coatings:** Nanocomposite coatings on buildings, windows, and solar panels create self-cleaning surfaces. Decomposing organic waste and impurities on these surfaces reduces maintenance costs and increases material durability.

Conclusion

This research describes how NiO-BS-GO nanocomposite improved photocatalytic materials. This nanocomposite is made by adding boron (B), sulfur (S), and graphene oxide (GO) to nickel oxide (NiO). Hydrothermal synthesis yielded a nanocomposite with improved photocatalytic capabilities, as shown by the degradation of methylene blue (MB) and rhodamine B (RhB) under visible light.

NiO-BS-GO nanocomposite photocatalytically breaks down organic dyes better. Due to its increased surface area, charge separation, and light absorption, the nanocomposite improves. Doping boosted the surface area and catalytic active sites of the nanocomposite, resulting in a BET surface area of 25.24 m^2/g. The nanocomposite was stable and reusable, making it ideal for long-term environmental rehabilitation. Boron (B) and sulfur (S) strengthened NiO, while graphene oxide (GO) provided a strong framework that inhibited particle aggregation and maintained a wide surface area.

NiO-BS-GO is ideal for wastewater treatment, air purification, solar-powered disinfection, soil remediation, and sustainable coatings due to its photocatalytic properties and durability. Degrading POPs, VOCs, and viruses makes this material versatile and effective in addressing environmental challenges. The study illuminated the mechanisms that improve photocatalytic activity. These approaches increase charge separation, surface area, and photocorrosion resistance. B and S doping with GO integration improved electron transport and reduced electron-hole recombination, improving photocatalytic performance.

Acknowledgement

We would like to acknowledge the PG department of chemistry Ranchi University Ranchi Jharkhand for kind support and providing technical support.

References

1. Chen Z, Xu YJ. Ultrathin TiO_2 layer coated-CdS spheres core-shell nanocomposite with enhanced visible-light photoactivity. ACS Appl Mater Interfaces. 2013;5(23):13353-13363.
2. Deng Y, Chen Y, Chen B, Ma J. Preparation, characterization and photocatalytic activity of $CuBi_2O_4/NaTaO_3$ coupled photocatalysts. J Alloys Compd. 2013;559:116-122.
3. Sudrajat H, Babel S. A new, cost-effective solar photoactive system N-ZnO@polyester fabric for degradation of recalcitrant compound in a continuous flow reactor. Mater Res Bull. 2016;83:369-378.
4. Sudrajat H, Babel S. An innovative solar photoactive system N-WO_3@polyester fabric for degradation of amaranth in a thin-film fixed-bed reactor. Sol Energy Mater Sol Cells. 2016;149:294-303.
5. Sudrajat H, Sujaridworakun P. Insights into structural properties of Cu species loaded on Bi_2O_3 hierarchical

structures for highly enhanced photocatalysis. J Catal. 2017;352:394-400.
6. He H, Yin J, Li Y, Zhang Y, Qiu H, Xu J, *et al*. Size controllable synthesis of single-crystal ferroelectric Bi4Ti3O12 nanosheet dominated with facets toward enhanced visible-light-driven photocatalytic activities. Appl Catal B Environ. 2014;156-157:35-43.
7. Liu L, Li Y, Yuan S, Ge M, Ren M, Sun C, *et al*. Nanosheet-based NiO microspheres: controlled solvothermal synthesis and lithium storage performances. J Phys Chem C. 2010;114(1):251-255.
8. Christy AJ, Umadevi M. Novel combustion method to prepare octahedral NiO nanoparticles and its photocatalytic activity. Mater Res Bull. 2013;48(12):4248-4254.
9. Granqvist CG. Handbook of Inorganic Electrochromic Materials. 1st ed. Amsterdam: Elsevier; c1995.
10. Loudon JC. Antiferromagnetism in NiO observed by transmission electron diffraction. Phys Rev Lett. 2012;109(26):267404.
11. Ji Z, Natu G, Wu Y. Cyclometalated ruthenium sensitizers bearing a triphenylamino group for p-type NiO dye-sensitized solar cells. ACS Appl Mater Interfaces. 2013;5(18):8641-8648.
12. Beak YW, An YJ. Microbial toxicity of metal oxide nanoparticles (CuO, NiO, ZnO, and Sb_2O_3) to Escherichia coli, Bacillus subtilis, and Streptococcus aureus. Sci Total Environ. 2011;409(8):1603-1608.
13. Wan X, Yuan M, Tie SL, Lan S. Effects of catalyst characters on the photocatalytic activity and process of NiO nanoparticles in the degradation of methylene blue. Appl Surf Sci. 2013;277:40-46.
14. Salavati-Niasari M, Mir N, Davara F. A novel precursor in preparation and characterization of nickel oxide nanoparticles via thermal decomposition approach. J Alloys Compd. 2010;493(1-2):163-168.
15. Wu L, Wu Y, Wei H, Shi Y, Hu C. Synthesis and characteristics of NiO nanowire by a solution method. Mater Lett. 2004;58(17-18):2700-2703.
16. Wang D, Xu R, Wang X, Li Y. NiO nanorings and their unexpected catalytic property for CO oxidation. Nanotechnology. 2006;17(4):979-983.
17. Alagiri M, Ponnusamy S, Muthamizhchelvan C. Synthesis and characterization of NiO nanoparticles by sol-gel method. J Mater Sci. Mater Electron. 2012;23(3):728-732.
18. Wu Z, Wang Y, Sun L, Mao Y, Wang M, Lin C. An ultrasound-assisted deposition of NiO nanoparticles on TiO2 nanotube arrays for enhanced photocatalytic activity. J Mater Chem A. 2014;2(21):8223-8229.
19. Anandan S, Lee GJ, Chen PK, Fan C, Wu JJ. Removal of orange II dye in water by visible light assisted photocatalytic ozonation using Bi2O3 and Au/Bi2O3 nanorods. Ind Eng Chem Res. 2010;49(20):9729-9737.
20. Bao DH, Chiu TW, Wakiya N, Shinozaki K, Mizutani N. Structural and electrical characteristics of chemical-solution-derived (Bi, La)$4Ti_3O_{12}$ thin films with various Bi2O3 template layers. J Appl Phys. 2003;93(1):497-503.
21. Leontie L. Optical properties of bismuth oxide thin films prepared by reactive magnetron sputtering. J Optoelectron Adv Mater. 2006;8(3):1221-1224.
22. Shuk P, Wiemhofer HD, Guth U, Gopel W, Greenblatt M. Oxide ion conducting solid electrolytes based on Bi2O3. Solid State Ionics. 1996;89(1-2):179-196.
23. Pan C, Li X, Wang F, Wang L. Synthesis of bismuth oxide nanoparticles by the polyacrylamide gel route. Ceram Int. 2008;34(2):439-441.
24. Xiaohong W, Wei Q, Weidong H. Thin bismuth oxide films prepared through the sol-gel method as photocatalyst. J Mol Catal A Chem. 2007;261(2):167-171.
25. Oudghiri-Hassani H, Rakass S, Al Wadaani FT, Al-ghamdi KJ, Omer A, Messali M, *et al*. Synthesis, characterization and photocatalytic activity of α-Bi_2O_3 nanoparticles. JTUSCI. 2015;9(4):508-512.
26. Pugazhenthiran N, Sathishkumar P, Murugesan S, Anandan S. Effective degradation of acid orange 10 by catalytic ozonation in the presence of Au-Bi_2O_3 nanoparticles. Chem Eng J. 2011;168(3):1227-1233.
27. Lin G, Tan D, Luo F, Chen D, Zhao Q, Qiud J, *et al*. Fabrication and photocatalytic property of α-Bi_2O_3 nanoparticles by femtosecond laser ablation in liquid. J Alloys Compd., 2010, 507(1).
28. Malathy P, Vignesh K, Rajarajan M, Suganthi A. Enhanced photocatalytic performance of transition metal doped Bi2O3 nanoparticles under visible light irradiation. Ceram Int. 2014;40(1):101-107.
29. Balachandran S, Swaminathan M. Facile fabrication of heterostructured Bi2O3-ZnO photocatalyst and its enhanced photocatalytic activity. J Phys Chem C. 2012;116(50):26306-26312.
30. Ye LQ, Zan L, Tian LH, Peng TY, Zhang JJ. The 001 facets-dependent high photoactivity of BiOCl nanosheets. Chem Commun. 2011;47(25):6951-6953.
31. Zhu LY, Xie Y, Zheng XW, Yin X, Tian XB. Oxidative catalytic cracking of n-butane to lower alkenes over layered BiOCl catalyst. Inorg Chem. 2002;41(18):4560-4566.
32. Zhang X, Ai ZH, Jia FL, Zhang LZ. Generalized one-pot synthesis, characterization, and photocatalytic activity of hierarchical BiOX (X = Cl, Br, I) nanoplate microspheres. J Phys Chem C. 2008;112(3):747-753.
33. Briand GG, Burford N. Bismuth compounds and preparations with biological or medicinal relevance. Chem Rev. 1999;99(9):2601-2658.
34. Armelao L, Bottaro G, Maccato C, Tondello E. Bismuth oxychloride nanoflakes: Interplay between composition-structure and optical properties. Dalton Trans. 2012;41(16):5480-5485.
35. Song JM, Mao CJ, Niu HL, Shen YH, Zhang SY. Hierarchical structured bismuth oxychlorides: self-assembly from nanoplates to nanoflowers via a solvothermal route and their photocatalytic properties. CrystEngComm. 2010;12(12):3875-3881.
36. Zhang KL, Liu CM, Huang FQ, Zheng C, Wang WD. Study of the electronic structure and photocatalytic activity of the BiOCl photocatalyst. Appl Catal B Environ. 2006;68(3-4):125-129.
37. Geng J, Hou WH, Lv YN, Zhu JJ, Chen HY. One-dimensional BiPO4 nanorods and two-dimensional BiOCl lamellae: fast low-temperature sonochemical synthesis, characterization, and growth mechanism. Inorg Chem. 2005;44(23):8503-8509.

38. Deng H, Wang J, Peng Q, Wang X, Li Y. Controlled hydrothermal synthesis of bismuth oxyhalide nanobelts and nanotubes. Chem Eur J. 2005;11(20):6519-6524.
39. Henle J, Simon P, Frenzel A, Scholz S, Kaskel S. Nanosized BiOX (X = Cl, Br, I) particles synthesized in reverse microemulsions. Chem Mater. 2007;19(3):366-373.
40. Peng HL, Chan CK, Meister S, Zhang XF, Cui Y. Shape evolution of layer-structured bismuth oxychloride nanostructures via low-temperature chemical vapor transport. Chem Mater. 2009;21(2):247-252.
41. Zhang X, Zhao L, Fan C, Liang Z, Han P. Effects of oxygen vacancy on the electronic structure and absorption spectra of bismuth oxychloride. Comput Mater Sci. 2012;61:180-184.
42. Shtarev DS, Makarevich KS, Shtareva AV, Blokh AI, Syuy AV. Application of pyrolitic method of synthesis for preparation of calcium bismuthate based photocatalyst. Proc SPIE. 2016;10176:101761L-2.
43. Hameed A, Gombac V, Montini T, Graziani M, Fornasiero P. Synthesis, characterization and photocatalytic activity of NiO–Bi2O3 nanocomposites. Chem Phys Lett. 2009;472(4-6):212-216.
44. Yang Q, Zhong J, Li J, Chen J, Xiang Z, Wang T, *et al*. Photo-induced charge separation properties of NiO/Bi2O3 heterojunctions with efficient simulated solar-driven photocatalytic performance. Curr Appl Phys. 2017;17(4):484-487.
45. Chai SY, Kim YJ, Jung MH, Chakraborty AK, Jung D, Lee WI. Heterojunctioned BiOCl/Bi2O3, a new visible light photocatalyst. J Catal. 2009;262(1):144-149.
46. Wang C, Shao C, Liuc Y, Zhang L. Photocatalytic properties BiOCl and Bi2O3 nanofibers prepared by electrospinning. Scr Mater. 2008;59:332–335.
47. Sun X, Zhang Y, Li P, Guo D, Zi H, Guo J, *et al*. Heterostructure nano-NiO/BiOCl composites with advanced adsorption and photocatalytic performance for organic dyes. J Alloys Compd. 2018;736:22–28.
48. Hao YJ, Li FT, Wang SS, Chai MJ, Liu RH, Wang XJ. One-step combustion synthesis of β-Bi2O3-NiO/Ni composites and their visible light photocatalytic performance. Mat Sci Eng B. 2014;186:41–47.
49. Shan LW, Wang GL, Liu LZ, Wu Z. Band alignment and enhanced photocatalytic activation for α-Bi2O3/BiOCl (001) core–shell heterojunction. J Mol Catal A: Chem. 2015;406:145–151.
50. Gao B, Chakraborty AK, Yang JM, Lee WI. Visible-light photocatalytic activity of BiOCl/Bi3O4Cl nanocomposites. Bull Korean Chem Soc. 2010;31:1941–1944.
51. Najafian H, Manteghi F, Beshkar F, Salavati-Niasari M. Efficient degradation of azo dye pollutants on ZnBi38O58 nanostructures under visible-light irradiation. Sep Purif Technol. 2018;195:30–36.
52. Shobeiri SA, Mousavi-Kamazani M, Beshkar F. Facile mechanical milling synthesis of NiCr2O4 using novel organometallic precursors and investigation of its photocatalytic activity. J Mater Sci Mater Electron. 2017;28:8108–8115.
53. Beshkar F, Khojasteh H, Salavati-Niasari M. Flower-like CuO/ZnO hybrid hierarchical nanostructures grown on copper substrate: glycothermal synthesis, characterization, hydrophobic and anticorrosion properties. Materials. 2017;10:697.
54. Zhu S, Yang C, Li F, Li T, Zhang M, Cao W. Improved photocatalytic Bi2WO6/BiOCl heterojunctions: One-step synthesis via an ionic-liquid assisted ultrasonic method and first-principles calculations. Mol Catal. 2017;435:33–48.
55. Zhijian L, Deqing W, Baocai L, Sheng CF, Xiuyun L. Preparation method for thermosetting pure polyester resin. CN101143921A; c2008.
56. Luo Y, Huang Q, Li B, Dong L, Fan M, Zhang F. Synthesis and characterization of Cu2O-modified Bi2O3 nanospheres with enhanced visible light photocatalytic activity. Appl Surf Sci. 2015;357A:1072-1079.
57. Zhao Q, Liu X, Xing Y, Liu Z, Du C. Synthesizing Bi2O3/BiOCl heterojunctions by partial conversion of BiOCl. J Mater Sci. 2017;52:2117–2130.
58. Lin S, Cui W, Li X, Sui H, Zhang Z. Cu2O NPs/Bi2O2CO3 flower-like complex photocatalysts with enhanced visible light photocatalytic degradation of organic pollutants. Catal Today. 2017;297:237–245.
59. Chen F, Yang Q, Wang S, Yao F, Sun J, Wang Y, *et al*. Efficient degradation of atrazine by mesoporous Bi2O2CO3 photocatalyst under visible light irradiation: performance and mechanism. Appl Catal B: Environ. 2017;200:180–190.
60. He W, Wang Y, Duan W, Ding J, Zhu M, Song L, *et al*. Effective degradation of different dyes over visible-light-driven BNNS/β-Bi2O3 composites. J Alloys Compd. 2018;749:447–456.
61. Wang X, Xu C, Li X, Zhang Q, Wang S, Niu Y, *et al*. Facile synthesis of 2D BiOCl/BiOI heterojunctions with improved visible light photoactivity. CrystEngComm. 2017;19:4070–4078.
62. He L, Cheng H, Hu J, Xie Y. Ultrathin Bi2O3 nanosheets: intermediate-microwave-assisted fast preparation and their application in photocatalysis. CrystEngComm. 2016;18:3775–3778.